RSC Advances

Insights into the fatty acid ester norethisterone enanthate binding to human albumin: fluorescence, circular dichroism, and docking investigations

Qing Wang, Xiangling Ma, Jiawei He, Yuanzhi Li, Hui Li[*]

Abstract: Norethisterone enanthate (NET-EN) is a fatty acid ester of norethisterone. The single crystallographic data of NET-EN [$a = 6.09236(14)$ Å, $b = 12.7347(3)$ Å, $c = 30.1234(8)$ Å, $\alpha = \beta = \gamma = 90°$, unit-cell volume $V = 2337.11$ Å^3, $Z = 4$, and space group $P2_12_12_1$] were obtained by using acetone as solvent. The interaction of NET-EN with human serum albumin (HSA) was investigated using different optical techniques and molecular modeling. The fluorescence quenching between NET-EN and HSA was a static quenching process. The fluorescence lifetime measurement provided us an insight into the occurrence of static quenching. Three commercially available steroid hormone drugs, namely, norethindrone, norethindrone acetate, and ethisterone, were weaker than NET-EN in terms of binding capability with HSA. Displacement experiments demonstrated that similar to progesterone, the binding site of NET-EN was mainly located in site 1 of HSA. Circular dichroism (CD) study showed that NET-EN had a minimal effect on the local conformation of HSA molecule. This study provided useful information for the better understanding and use of NET-EN.
Keywords: norethisterone enanthate, single crystal X-ray diffraction, human serum albumin (HSA), interaction

1. Introduction

Steroidal compounds display a variety of biological functions and play an important role in life[1]. Steroidal drugs are widely used in traditional medicines, such as contraception. According to public information, an estimated 222 million women in developing countries prefer to delay or stop childbearing but are not using any method of contraception. Using contraceptives is an advanced method recommended by the World Health Organization (WHO). Commercially available contraceptives can be divided into emergency contraceptive, immediate–acting contraceptive, short-acting contraceptive, and long-acting contraceptive, among others. Today, millions of women worldwide use injectable steroid formulation progestin-only injectable and combined monthly contraceptive[2]. Norethisterone enanthate (NET-EN) is a widely used injectable preparation in many countries[3, 4]. It is a fatty acid ester of norethisterone (NET). Usually, NET-EN is prepared from NET and enanthic anhydride by esterification in presence of 4-dimethylaminopyridine (Fig. 1)[5]. NET-EN has weak androgenic and estrogenic activities[6]. Fatty acid esters of steroids are known to have longer half-life compared with the parent compound[7]. NET-EN

College of Chemical Engineering, Sichuan University, Chengdu 610065, People's Republic of China. E-mail: lihuilab@sina.com; Fax: +86 028 85401207; Tel: +86 028 85405149.

results in high suppression of spermatogenesis, which could be attributed to its additional direct effect on testis[8]. In men, a single injection of 200 mg NET-EN immediately leads to profound and significant suppression of serum luteinizing hormone, follicle-stimulating hormone, testosterone, and sex hormone binding globulin, as well as rapid suppression of spermatogenesis[9].

When NET-EN is injected into veins clinically, NET-EN either binds to plasma proteins and lipids or is freely available[10]. Plasma protein binding (PPB) is considered an important parameter throughout an ongoing drug-development program[11, 12]. Human serum albumin (HSA) has been the most widely used model protein to evaluate drug–protein systems because of the high concentration of albumin in human blood plasma[13, 14]. HSA has multiple hydrophobic binding sites and binds a diverse set of drugs and hormones[15, 16]. Crystallographic analyses of HSA have revealed that protein contains three homologous α-helical domains (I–III), namely, I (residues 1–195), II (residues 196–383), and III (residues 384–585), which are further divided into a pair of subdomains termed "A" and "B." By using natural mutants of HSA, Kragh-Hansen *et al.* indicated the high-affinity binding site of representative steroids–testosterone and progesterone to be located in domain II[17]. Recently, Ferenc Zsila pointed out that they were located in subdomain IIA by employing a circular dichroism (CD) spectroscopic approach[18]. Molecular recognition and binding of ligands (atoms, ions, and molecules) by proteins with high sensitivity and selectivity are of central importance to all biomolecular processes and of key importance for the basic and applied sciences.

The Special Program on Research on Human Reproduction of the WHO once prepared and tested a number of esters of NET to improve long-acting progestational compounds[19]. NET-EN was chosen for comparison. Protein binding in blood is an important factor in the transport and release[20]. In-depth understanding and analysis of NET-EN and its interaction with HSA are essential and will significantly promote medical purposes[21–23]. In the present work, crystalline NET-EN was obtained and studied by single crystal X-ray diffraction. This study is necessary for the better understanding of NET-EN from the atomic level. Several spectroscopic methods and molecular docking were used to investigate the interaction of NET-EN with HSA. Fluorescence spectrometry was used to determine the binding affinity of NET-EN to HSA and to investigate the thermodynamics of their interaction. In view of the nature and magnitude of drug–protein interaction influencing the biological activity of the drug[24], we performed measurements and docking computations to compare the binding affinity between NET-EN and the three structures similar to steroid hormone drugs under physiological conditions. Given that NET-EN is a synthetic progestagenic compound, it may share the same high-affinity binding site with progesterone. Thus, displacement experiments along with molecular docking were performed to establish the main binding sites of HSA. The binding of a drug to a protein may affect the conformation and the stability of that protein. Thus, CD was used. This study may provide valuable information about NET-EN and may serve as a reference in drug designing.

2. Materials and methods

2.1. Preparation of stock solution

HSA (essentially fatty acid free), with an assumed molecular weight of 66,500, was purchased from Sigma-Aldrich Company (St. Louis, USA). The stock solutions (2.0×10^{-5} M) were prepared in Tris-HCl buffer with pH value of 7.40 and 0.1 M NaCl. NET-EN, NET, norethindrone acetate (NET-AC), and ethisterone (ET) were purchased from Xiya Reagent Co., Ltd. (Chengdu, China). Warfarin and ibuprofen were purchased from J&K Scientific Ltd. (Beijing, China). NET-EN, warfarin, and ibuprofen were dissolved in anhydrous ethanol to obtain 2.0×10^{-3} M stock solution, which was then stored at 0 °C to 4 °C.

2.2 Instrumental methods

Fluorescence measurements were conducted on a Cary Eclipse fluorescence spectrophotometer (Varian, USA) equipped with 1.0 cm quartz cells. HSA concentration was kept at 2.0 μM, and NET-EN concentration varied from 0 μM to 48.0 μM on the basis of preliminary experiments. Fluorescence spectra were measured using 10/5 nm (excitation/emission) slit widths. The excitation wavelength was fixed at 280 nm. The fluorescence spectra were recorded in the 300 nm to 500 nm range at 298, 304, and 310 K.

Fluorescence lifetime measurements were executed using a Horiba Jobin Yvon FluoroMax-4 spectrofluorometer (HORIBA, FRA). The time-resolved HSA fluorescence quenching by the drug was recorded by fixing 280 nm as the excitation wavelength and 338 nm as the emission wavelength. The HSA concentration was fixed at 2.0×10^{-6} mol·L^{-1}, and NET-EN concentration was varied from 1.6×10^{-5} mol·L^{-1} to 4.8×10^{-5} mol·L^{-1} at room temperature.

To evaluate the effect of ethanol on HSA conformation and fluorescence quenching, 2.0 mL of 1.0 μM HSA was titrated with 0.1% to 1.0% (V/V) ethanol during the monitoring of UV-vis and fluorescence spectra. No changes were observed in the spectral profiles (data not shown), which indicated that the conformation of HSA did not change in the presence of 0.1% to 1.0% (V/V) ethanol, and the effects of ethanol on the structural changes in HSA were not significant. In this study, all fluorescence intensities were corrected for the absorption of excited light and the re-absorption of emitted light. The following relationship was used to correct the inner-filter effect[25]:

$$F_{corr} = F_{obs} \times e^{\frac{A_{ex} + A_{em}}{2}} \tag{1}$$

where F_{corr} and F_{obs} are the corrected and observed fluorescence intensities, respectively; A_{ex} and A_{em} are the absorption of the system at the excitation and emission wavelengths, respectively.

CD spectra were recorded on a CD spectrometer (Model 400, AVIV, USA). CD measurements were conducted with a constant HSA concentration of 2.0 μM, whereas complex concentration was varied from 0 μM to 10.0 μM [ri = (NET-EN)/(HSA) = 0:1, 5:1, 10:1]. Spectra were recorded at 298 K in a 2 mm quartz cell from 250 nm to 200 nm with a step size of 1 nm, a band width of 1 nm,

and an averaging time of 0.5 s.

2.3. Molecular modeling preparation

Discovery Studio 3.1 (DS 3.1; Accelrys Co., Ltd., US) was provided by the State Key Laboratory of Biotherapy (Sichuan University, China). The crystal structures of HSA (PDB ID: 2BXD and 2BXG) were obtained from a protein data bank for docking simulations. Both 2BXD and 2BXG contained two chains. However, 2BXD contained only warfarin, whereas 2BXG contained only ibuprofen. Chain A was deleted from 2BXD and 2BXG. Hybridization states, charges, and angles were assigned in the protein structure with missing bond orders. Explicit H atoms were added at pH 7.40. The energy of the protein structure was minimized in 200 steps of the smart minimize method. To prepare ligands, we generated the 3D structure of NET-EN by using ChemBioOffice 2010[26]. We then optimized the structure with DS 3.1. CDOCKER docking programs implemented in DS 3.1 were used in this study[27].

3. Results and discussion

3.1. Single-crystal X-ray diffraction

Crystallization of NET-EN at room temperature was successful using acetone as solvent. X-ray diffraction data for NET-EN were collected on a New Gemini, Dual, Cu at zero, EosS2 diffractometer. The crystal was kept at 110.01(16) K during data collection. The structure was solved with olex2[28], a structure solution program using charge flipping and refined with the ShelXL refinement package using least squares minimization[29]. A figure was drawn with ORTEP-3. Crystal and experimental data are listed in Table 1, and the corresponding structures are shown in Fig. 2. Crystallographic data for NET-EN were deposited with the Cambridge Crystallographic Data Center with a supplementary publication number of CCDC-1030994. Copies of the data can be obtained free of charge on application to CCDC, 12 Union Road, Cambridge CB2 1EZ, United Kingdom (e-mail: deposit@ccdc.cam.ac.uk).

In the crystal structure, molecules were arranged in a head-to-tail fashion. The molecular conformation of NET-EN contained six chiral centers (Fig. 3). In the molecular structure, ring A had an intermediate sofa-half-chair conformation[30]. Rings B and C had chair conformations, and ring D adopted envelope conformation[31]. Unlike NET-AC[32], NET-EN was arranged without intramolecular and intermolecular H bonding. From the comparison of the bond lengths (Å) and angles (°) of NET-EN and NET-AC (Table 2), the bond lengths of ethynyl residues C(6)–C(14) and C(7)–C(30) almost unchanged if the error was considered. They remained strong H-bond donors. The strong steric hindrance of heptanoic acid side chain hindered the formation of H bonds, although C(26)–O(3) and C(10)–O(2) were strong acceptors.

3.2. Fluorescence-quenching measurements

The fluorescence intensity decreased when HSA concentration was fixed at 2.0×10^{-6} M at room temperature after the addition of NET-EN, as shown in Fig. 4. This finding suggested that an interaction occurred between NET-EN and HSA. The intrinsic fluorescence of HSA was generally caused by tryptophan (Trp-214 in HSA)

and tyrosine (17 Tyrs in HSA) because phenylalanine had a low quantum yield[33]. Only tryptophanyl residues were excited at 295 nm, whereas the excitation at 280 nm also excited tyrosil groups[34]. The inset in Fig. 4 shows that the quenching curve with λ_{ex} = 280 nm did not overlap the curve with λ_{ex} = 295 nm. Consequently, both types of fluorophore may participate in NET-EN–HSA interaction.

Fluorescence quenching is the decrease of the quantum yield of fluorescence from a fluorophore. Quenching can be caused by different mechanisms, such as dynamic and static quenching. The well-known Stern–Volmer equation can be used to validate the quenching mechanism by analyzing the fluorescence data at different temperatures, i.e.,

$$F_0/F = K_{SV}[Q] + 1, \tag{2}$$

where F_0 and F are the fluorescence intensities in the absence and presence of the quencher, respectively; K_{SV} is the Stern–Volmer quenching constant. Table 3 summarizes the calculated K_{SV} at 298, 310, and 315 K. Dynamic quenching and static quenching are caused by diffusion and ground-state complex formation, respectively. The dynamic quenching constants are expected to increase with increasing temperature because they depend on diffusion. A high temperature decreases the complex stability, thereby resulting in a low static quenching constant[35]. K_{SV} decreased gradually with increasing temperature. Thus, quenching may follow a static mechanism and was due to complexation.

Time-resolved fluorescence spectroscopy is a tool that can probe the interaction between ligands and proteins. Using fluorescence lifetime measurements can distinguish static quenching from dynamic quenching[35]. Formation of static ground-state complexes does not decrease the decay time of the uncomplexed fluorophores. Dynamic quenching is a rate process that acts on the entire excited-state population and thus decreases the mean decay time of the entire excited-state population. Time-resolved fluorescence lifetime measurement was conducted to substantiate the static quenching mechanism between HSA and NET-EN. The data were analyzed by tail fitting method. The qualities of the fits were assessed by χ^2 values and residuals. Mean (average) fluorescence lifetimes (⟨τ⟩) for biexponential iterative fitting were calculated from the decay times and the pre-exponential factors (α) by using the following relation[36]:

$$⟨τ⟩ = α_1τ_1 + α_2τ_2. \tag{3}$$

We chose the mean fluorescence lifetime as an important parameter to explore the behavior of HSA molecular bound to NET-EN. The lifetime data showed that the average lifetime of the fluorophore of HSA decreased marginally from 6.267 ns to 5.762 ns with increasing NET-EN (Table 4). The bound NET-EN may directly influence the lifetime of fluorophore. The observed fluorescence was from the uncomplexed fluorophores. Table 4 exhibits a tiny decrease in the average lifetime of uncomplexed fluorophores with increasing concentration of NET-EN. Such a change of the average fluorescence lifetime in tested systems suggested the formation of complex between the NET-EN and HSA. Fluorescence quenching was a static mechanism because of ground-state complex formation, which was consistent with the fluorescence quenching analysis results.

3.3 Binding parameters and mode

Given that NET-EN-induced fluorescence quenching of HSA was a static process, the binding constant (K) and the number of bound complexes to HSA (*n*) were determined by plotting the double-logarithm regression curve of the fluorescence data by using the following "modified" Stern–Volmer equation:

$$\log(F_0 - F)/F = \log K + n\log[Q], \tag{4}$$

where K is the binding constant of the site, and n is the binding site multiplicity per class of binding site. The results are summarized in Table 5. The values of K suggested a strong binding force between NET-EN and HSA. The value of n (approximately equal to 1) suggested the presence of a single high-affinity binding site existing in HSA.

The thermodynamic parameters of the binding reaction comprised the major evidence that confirmed the intermolecular forces. Enthalpy change (ΔH^0) and entropy change (ΔS^0) can help confirm the binding modes. ΔH^0 and ΔS^0 can be calculated using the van't Hoff equation as follows[37]:

$$\ln K = -\frac{\Delta H^0}{RT} + \frac{\Delta S^0}{R}, \tag{5}$$

where K is analogous to the associative binding constants at the corresponding temperature, and R is the gas constant. The free-energy change (ΔG^0) can be estimated as follows:

$$\Delta G^0 = \Delta H^0 - T\Delta S^0 = -RT\ln K. \tag{6}$$

The results are presented in Table 5. The negative ΔG^0 values indicated that the binding of NET-EN with HSA occurred spontaneously. Four representative interaction forces, namely, hydrophobic force, H bond, van der Waals force, and electrostatic interactions, existed between small molecular substrates and biological macromolecules generally. According to the theory of Ross and Subramanian[38], negative ΔH^0 and negative ΔS^0 values indicated that H bonding, along with the van der Waals forces, played major roles in the binding between NET-EN and HSA.

3.4 Comparative study of similar structures

NET, NET-AC, and ET are three commercially available steroid hormone drugs. These drugs are similar to NET-EN in structure and function (Fig. 5). PPB model, implemented by DS 3.1, was used to predict the four compounds. PPB determines whether a compound is likely to be highly bound to the carrier proteins in the blood on the basis of AlogP98 and the 1D similarity between two sets of "marker" molecules. One set of markers is used for flag binding at a level of 90% or greater, and the other set is used for flag binding at a level of 95% or greater. Each marker molecule has a characteristic of 1D similarity threshold that is used to determine whether a given compound is sufficiently similar that it binds at the associated level of the marker (90% or 95%). Therefore, if a compound exhibits 1D similarity to any 90% marker molecule that meets or exceeds the marker threshold, then the compound is likely to bind at 90% or higher. Binding at 95% or greater is predicted if the similarity threshold is exceeded for any marker in the 95% set[39, 40]. In this study, the results indicated that the PPB level of NET-EN was 2 [binding was >95% (flagged at

95% or AlogP98 >5.0)], whereas those of NET, NET-AC, and ET were 1 [binding was >90% (flagged at 90% or AlogP98 >4.0)]. Hence, NET-EN was more likely to be highly bound to carrier proteins in the blood than NET, NET-AC, and ET. Although carrier proteins in the blood do not have an equal amount of HSA, HSA remains the most abundant protein in human blood plasma ascribed to drug-binding and transport properties. Therefore, the PPB results in this study could provide a good reference that NET-EN bound stronger to HSA than NET, NET-AC, and ET. PPB model is based on the published QSAR models to compute and analyze plasma protein-binding properties. The structure differentiations among NET, NET-AC, and ET are significantly less than NET-EN. Thus, distinguishing the binding ability of NET, NET-AC, and ET based on a rough prediction is difficult.

Interference experiments of similar steroids were further performed by keeping the binary mixture of NET-EN–HSA complex in 1:1 ratio. The percentage (I_{per}) of the initial fluorescence with distractors was calculated as follows:

$$I_{per}= F/F_0, \tag{7}$$

where F and F_0 represent the fluorescence intensities of NET-EN–HSA in the absence and presence of the probe, respectively. The changes induced by similar steroids are presented in Fig. 5. The binary mixture of NET-EN–HSA complex molecules was affected at different extents. NET had almost no influence with the increase in concentration. The downward trend of I_{per} shows that the other two steroids (NET-AC and ET) competed with NET-EN to a certain extent. ET had more influence than NET-AC on the binary mixture. On the whole, the influences caused by NET, NET-AC, and ET were limited, especially when they were in low concentrations. NET, NET-AC, and ET were weaker than NET-EN in the binding capability with HSA. This result was consistent with the prediction. At the same time, based on different influence extents on the binary mixture, we could ascertain that the binding ability was NET-EN>ET>NET-AC>NET. Assuming that NET is the parent structure, the presence of R_1 and R_2 (Fig. 5) promoted the binding ability. In addition, the binding ability had no connection with the position of R_1 and R_2, but the substituent itself.

Among the steroids, NET-EN and NET-AC were both fatty acid esters of NET. In practical application, ET-AC is usually used as a short-acting oral contraceptive, whereas NET-EN is usually used as a two-month intramuscular injectable preparation for long-acting contraception. NET-EN is also biologically active and effective in inhibiting fertility if taken orally[22]. After absorption, NET-AC is rapidly and completely deacetylated to NET, but NET-EN is stored and slowly released. Finally, NET-AC and NET-EN are hydrolyzed to NET mainly in the liver with the help of the bloodstream because neither muscle nor plasma causes significant breakdown of ester in humans[41]. Through nonspecific binding, HSA acts as a plasma carrier to help the hydrophobic steroid hormones across organ–circulatory interfaces and then release them to tissues[42]. However, the fractions of steroids that bind with high affinity to HSA are less easily available to tissues[43]. In this study, NET-AC was weaker in binding capability with HSA than NET-EN. Strong binding to HSA decreased high concentrations of free ligands released to the liver. The efficiency of converting

NET-EN to NET will inevitably become weaker than that of NET-AC conversion to NET under the same conditions.

3.5 Identification of the binding site

Sudlow *et al.* suggested two main distinct binding sites on HSA, namely, sites 1 and 2[44]. Warfarin can bind specifically to site 1, which is located in subdomain IIA. Site 2 of HSA, which is located in subdomain IIIA, displays affinity with ibuprofen[45]. The residues of sites 1 and 2 on the protein are the key determinants of binding specificity. Although few ligands are found to be bounded in one or several of these secondary binding sites, these substances are usually bound to site 1 or 2 or both sites[17]. Displacement experiments were performed using warfarin and ibuprofen as site probes to establish the main binding site in HSA for NET-EN. The binding constants in the presence of warfarin and ibuprofen were calculated using Eq. (3). The K values obtained were $(2.836 \pm 0.0158) \times 10^3$ L·mol^{-1} (R = 0.9963) and $(9.911 \pm 0.0137) \times 10^3$ L·mol^{-1} (R = 0.9976) for warfarin and ibuprofen, respectively. The large decrease in K values $(1.053 \pm 0.0035) \times 10^4$ L·mol^{-1} (R = 0.9967) for warfarin suggested that NET-EN and progesterone were mainly bound to site 1 of HSA.

The CDOCKER docking program (a molecular dynamic simulated-annealing-based algorithm) was selected to determine whether NET-EN can bind to site 1 of HSA[46, 47]. CDOCKER is a grid-based molecular docking method that employs CHARMm[48, 49]. Specifying the ligand placement in the active site is possible by using a binding site sphere. In this study, 2BXD/2BXG was defined as the total receptor, and the site sphere was built with a diameter of 2.5 Å on the basis of warfarin/ibuprofen[6]. In 2BXD, warfarin clustered in the center of site 1 pocket. In 2BXG, ibuprofen clustered in the center of the binding pocket of site 2 and oriented with at least one O atom in the vicinity of the polar patch. During docking, a freshly prepared NET-EN was added. CHARMm was selected as force field. Pre-existing warfarin/ibuprofen was then removed. The heating steps were set as 2000 K, and the heating target temperature was 700 K. The cooling steps were set as 5000 K, with a cooling target temperature of 300 K. Ten molecular docking poses that were saved for each site were ranked according to −CDOCKER energy (−E$_{CD}$, kcal/mol). This score included internal ligand strain energy and receptor-ligand interaction energy and was used to sort the poses of each input ligand. The pose with the highest −E$_{CD}$ was chosen as the most suitable pose for the subsequent pose analysis.

The results showed that NET-EN had 10 docking poses in site 1 but contained no docking poses in site 2. Thus, the binding of NET-EN mainly to site 1 was confirmed. Fig. 6 shows that NET-EN was well inserted into the hydrophobic cavity of the active site (site 1). NET-EN molecule was mainly surrounded by Tyr-150, Lys-195, Lys-199, Trp-214, Ala-215, Arg-218, Leu-219, Arg-222, Leu-238, Val-241, Ala-291, etc. The parent structure of NET-EN pinned snugly between the apolar side-chains of Leu-238 and Ala-291. This group was evident at the mouth of the pocket, where a wide opening existed that provided a significant room for movement. Then we used the same method to obtained the most suitable poses of NET, NET-AC, and ET. They also attached well between the polar side-chains of Leu-238 and Ala-291 (Fig. 7).

NET and NET-AC almost overlapped with NET-EN. Their tails were consistently toward Trp-214, an important fluorophore in HSA. Differently, the tail of ET had an opposite direction (inset in Fig. 7). The longer and more flexible heptanoic acid side chain of NET-EN was closer to Trp-214 and more likely had an effect on the fluorophore. Time-resolved fluorescence study (section 3.2) had shown the bound NET-EN directly influenced the lifetime of fluorophore. The heptanoic acid side chain should be the main factor. Gaps in the active site of NET-EN–HSA complex were not favorable. When NET-EN was inserted into HSA, HSA and NET-EN underwent changes to minimize the space along with the van der Waals forces[50]. Among the four steroids, the existence of R_1 and R_2 can reduce this space to a certain extent. Their existence is favorable to for the better fit of small molecules to HSA. The Lys-199 residue of HSA was capable of forming intermolecular H bonds with O(1). Arg-222 also formed a H bond with O(2). These two H bonds between NET-EN and HSA were in agreement with the binding mode proposed in thermodynamic analysis. The importance of H bonding in the process of NET-EN–HSA complex was to balance the adverse energetic effects caused by water displacement. In this study, H bonding was an important contributor to complex stability. These results can serve as bases to explain the efficient fluorescence quenching of HSA emission in the presence of NET-EN. H bonding is indispensable in the formation of both secondary and tertiary structures of proteins. The 3D structures and functions of many biological molecules are highly dependent on intramolecular H bonding. The newly formed H bonding may affect the original bonding. We further explored the secondary structure of HSA, i.e., whether it was affected by NET-EN.

3.6 CD spectroscopy studies

CD is a universally acknowledged technique used for the structural characterization of proteins. To investigate the effect of NET-EN binding on the conformation change in HSA, CD spectroscopic analysis was performed on free HSA and on NET-EN–HSA complex. Fig. 8 shows that HSA exhibited two negative ellipticities at 208 and 220 nm, which were the characteristics of the α-helix structure of proteins[51]. The shapes of CD spectra were similar with and without NET-EN, which suggested that HSA structure was also predominantly α-helix. However, the negative bands were not shifting, and the intensity decreased slightly. CD results were generally expressed in terms of mean residue ellipticity (MRE) in $\text{deg}\cdot\text{cm}^2\cdot\text{dmol}^{-1}$ according to the following equation:

$$MRE = \frac{\text{observed CD(m deg)}}{10 C_p n l}, \tag{8}$$

where C_p is the molar concentration of the protein, n is the number of amino acid residues (585 for HSA), and l is the path-length of the cell (here, 2 nm). The α-helix contents of free and combined HSA were calculated from the MRE values at 208 nm through the following equation:

$$\alpha - \text{helixl}(\%) = \left(\frac{-\text{MRE}_{208} - 4000}{33000 - 4000} \right) \times 100 .\tag{9}$$

However, X-ray structural analysis showed higher α-helix content for HSA (67%) than those obtained by spectroscopic methods[52]. The reason can be due to the sample preparation and the protein structural arrangements in the solution (spectroscopy). However, these factors do not affect the change tendency of secondary structure. At present, the *α*-helix estimated by many studies is around 60%[53, 54]. We calculated that the native HSA solution had a 55.57% *α*-helix structure. This result was in agreement with the values reported by other investigators. The α-helix content of HSA decreased to 55.06% and 54.11% upon the addition of NET-EN with molar concentration ratios of 1:5 and 1:10. The fact that its *α*-helix content decreased minimally indicated that NET-EN had a minimal effect on the secondary structure of HSA. This phenomenon also has appeared in Shi's study on the interaction of megestrol acetate with BSA[55]. Hydrogen bonding is necessary to form secondary and tertiary protein structures. The original bonding of HSA was almost unaffected when NET-EN was inserted into HSA.

Conclusions

This paper reports the single crystallographic data of NET-EN obtained by using acetone as solvent. These data will help us better understand the physical and chemical properties of NET-EN. The strong steric hindrance of heptanoic acid side chain hindered the formation of H bonds, although strong acceptors were present. This paper also demonstrates a detailed investigation of the interaction between NET-EN and HSA. The experimental data showed that NET-EN could insert into HSA and quench the intrinsic fluorescence of HSA by static mechanism, which was induced by the formation of NET-EN–HSA complex. The existence of static quenching mechanism was confirmed by time-resolved fluorescence spectral analysis. H bonding, along with the van der Waals forces, played major roles in the binding between NET-EN and HSA. H bonding was an important contributor to the stability of the complex. Interference experiments and PPB model showed that NET, NET-AC, and ET were weaker than NET-EN in combination with HSA. NET had the weakest binding ability among the four steroids. The binding ability had no connection with the position of substituent, but the substituent itself. The existence of substituents in NET can reduce this space to a certain extent, which helps in the better fit of small molecules to HSA. Particularly, NET-AC was weaker in binding capability than NET-EN. Strong binding decreases high concentrations of NET-EN in plasma. NET-AC converted NET more efficiently than NET-EN did. From the binding capability perspective, this conclusion was in accordance with the actual medical application. Displacement experiments demonstrated that the binding site of NET-EN was mainly located in site 1 of HSA. The parent structure of NET-EN pinned snugly between the apolar side-chains of Leu-238 and Ala-291, providing a significant room for movement. This phenomenon is advantageous for the binding of large molecules to HSA. Comprehensive time-resolved fluorescence study results and docking results

showed that the tail of NET-EN was close to Trp-214 and had an effect on the lifetime of fluorophore. Conformation study showed that NET-EN had an insignificant effect on the local conformation of HSA molecule. The original bonding of HSA was almost unaffected when NET-EN was inserted into HSA. This study is expected to provide insights into the protein binding of NET-EN and is useful for the better utilization of NET-EN in the standardized screening of pharmaceutical firms and for clinical research.

Acknowledgements

References

1. F. Zeelen, *Prin. Med. Biol.,* 1997, 8, 427-463.

2. T. E. Canto de Cetina, M. O. Luna, J. A. Cetina Canto and S. Bassol, *Contraception*, 2004, 69, 115-119.

3. A. Junaidi, C. M. Luetjens, J. Wistuba, A. Kamischke, C. H. Yeung, M. Simoni and E. Nieschlag, *Eur. J. Endocrinol.*, 2005, 152, 655-661.

4. A. Qoubaitary, C. Meriggiola, C. M. Ng, L. Lumbreras, S. Cerpolini, G. Pelusi, P. D. Christensen, L. Hull, R. S. Swerdloff and C. Wang, *J. Androl.*, 2006, 27, 853-867.

5. G. Q. Wang, F. Lin, Z. Y. Wang and Y. G. Wu, *Chinese J.Pharmaceuticals*, 2008, 39, 9-10.

6. P. Ravinder, K. Madhavan Nair and B. Sivakumar, *Indian J. Physiol. Pharmacol.*, 1998, 42, 485-490.

7. K. Fotherby and F. James, *Adv. Steroid Biochem. Pharmacol.*, 1972, 3, 67-165.

8. A. Kamischke, J. Diebäcker and E. Nieschlag, *Clin. Endocrinol.*, 2000, 53, 351-358.

9. A. Kamischke, D. Plöger, S. Venherm, S. Von Eckardstein, A. Von Eckardstein and E. Nieschlag, *Clin. Endocrinol.*, 2000, 53, 43-52.

10. H. X. Zhang and Y. Liu, *Steroids*, 2014, 80, 30-36.

11. M. L. Howard, J. J. Hill, G. R. Galluppi and M. A. McLean, *Comb. Chem. High T. Scr.*, 2010, 13, 170-187.

12. B. Buscher, S. Laakso, H. Mascher, K. Pusecker, M. Doig, L. Dillen, W. Wagner-Redeker, T. Pfeifer, P. Delrat and P. Timmerman, *Bioanalysis*, 2014, 6, 673-682.

13. J. Wei, F. Jin, Q. Wu, Y. Jiang, D. Gao and H. Liu, *Talanta*, 2014, 126, 116-121.

14. A. A. Bhattacharya, T. Grüne and S. Curry, *J. Mol. Biol.*, 2000, 303, 721-732.

15. J. Ghuman, P. A. Zunszain, I. Petitpas, A. A. Bhattacharya, M. Otagiri and S. Curry, *J. Mol. Biol.*, 2005, 353, 38-52.

16. A. J. Ryan, J. Ghuman, P. A. Zunszain, C. W. Chung and S. Curry, *J. Mol. Biol.*, 2011, 174, 84-91.

17. U. Kragh-Hansen, L. Minchiotti, S. O. Brennan and O. Sugita, *Eur. J. Biochem.*, 1990, 193, 169-174.

18. F. Zsila, *Mol. Pharm.*, 2013, 10, 1668-1682.

19. G. Bialy, R. Blye, R. Enever, R. Naqvi and M. Lindberg, *Steroids*, 1983, 41, 419-439.

20. G. Van Os, E. Ariens, A. Simonis and E. Ariens, 1Academic Press, New York, 1964.

21. G. U. Nienhaus, *Protein-Ligand Interactions*, Springer, 2005.

22. P. Ravinder, V. Shatrugna, K. M. Nair and B. Sivakumar, *Contraception*, 1997, 55, 373-379.

23. H. G. Brittain, *Polymorphism in pharmaceutical solids*, CRC Press, 2009.

24. Z. Chen, H. Xu, Y. Zhu, J. Liu, K. Wang, P. Wang, S. Shang, X. Yi, Z. Wang, W. Shao and S. Zhang, *RSC Adv.*, 2014, 4, 25410.

25. J. Yan, G. Zhang, J. Pan and Y. Wang, *Int. J. Biol. Macromol.*, 2014, 64, 213-223.

26. CATALYST version 4.11, Users' Manual. San Diego: Accelrys Software Inc.; 2005

27. Q. Wang, J. He, J. Yan, D. Wu and H. Li, *Luminescence*, 2015, 30, 240-246.

28. G. M. Sheldrick, *Acta Crystallogr. A*, 2008, 64, 112-122.

29. C. B. Hubschle, G. M. Sheldrick and B. Dittrich, *J. Appl. Crystallogr.*, 2011, 44, 1281-1284.

30. Z. Gałdecki, P. Grochulski, Z. Wawrzak and W. L. Duax, *J. crystallogr. spectroscopic res.*, 1989, 19, 941-947.

31. H. Li, H. Qian, J. Li and S. Ma, *J Chem. Crystallogr.*, 2011, 41, 1208-1213.

32. T. Steiner, *Acta Crystallogr C*, 1996, 52, 2261-2263.

33. Q. Wang, J. Yan, J. He, K. Bai and H. Li, *J. Lumin.*, 2013, 138, 1-7.

34. J. Równicka-Zubik, L. Sułkowski, M. Maciążek-Jurczyk and A. Sułkowska, *J. Mol. Struct.*, 2013, 1044, 152-159.

35. J. R. Lakowicz, Principles of fluorescence spectroscopy, Springer, 2009.

36. D. Xiao, L. Zhang, Q. Wang, X. Lin, J. Sun and H. Li, *J. Lumin.*, 2014, 146, 218-225.

37. R. G. Mortimer, *Physical Chemistry*, Elsevier, 2008.

38. P. D. Ross and S. Subramanian, *Biochemistry*, 1981, 20, 3096-3102.

39. S. L. Dixon and K. M. Merz, J. Med. Chem., 2001, 44, 3795-3809.

40. J. He, Q. Wang, L. Zhang, X. Lin and H. Li, *J. Lumin.*, 2014, 154, 578-583.

41. D. Back, A. Breckenridge, C. R. Chapman, F. E. Crawford, K. A. Olsen, M. E. Orme and P. Rowe, *Contraception*, 1981, 23, 125-132.

42. W. M. Pardridge, *Endocr. Rev.*, 1981, 2, 103-123.

43. A. Mooradian, D. Pamplona, S. Viosca and S. Korenman, *J. Steroid Biochem.*, 1988, 29, 369-370.

44. G. Sudlow, D. Birkett and D. Wade, *Mol. Pharmacol.*, 1975, 11, 824-832.

45. G. Sudlow, D. Birkett and D. Wade, *Mol. Pharmacol.*, 1976, 12, 1052-1061.

46. M. Vieth, J. D. Hirst, A. Kolinski and C. L. Brooks, *J. Comput. Chem.*, 1998, 19, 1612-1622.

47. G. Wu, D. H. Robertson, C. L. Brooks and M. Vieth, *J. Comput. Chem.*, 2003, 24, 1549-1562.

48. Y. Dai, N. Chen, S. Jia, Q. Wang, Dong, Lilong, Zheng, Heng , Zhang, Xiuli and D. Feng, *Iran. J. Pharm. Res.*, 2012, 11, 807-830.

49. Q. Wang, J. He, D. Wu, J. Wang, J. Yan and H. Li, *J. Lumin.*, 2015, 164, 81-85.

50. A. C. A. Roque, *Ligand-Macromolecular Interactions in Drug Discovery*, Springer 2010.

51. V. D. Suryawanshi, P. V. Anbhule, A. H. Gore, S. R. Patil and G. B. Kolekar, *J. Photoch. Photobio. B*, 2013, 118, 1-8.

52. X. M. He and D. C. Carter, *nature*, 1992, 358, 209-215..

53. N. Shahabadi, S. Hadidi and F. Feizi, *Spectrochim. Acta. A.,* 2015, 138, 169-175.

54. N. Kishikawa, K. Ohyama, A. Saiki, A. Matsuo, M. F. Ali, M. Wada, K. Nakashima and N. Kuroda, *Anal. Chim. Acta*, 2013, 780, 1-6.

55.　　　J. H. Shi, Y. Y. Zhu, J. Wang and J. Chen, *Luminescence*, 2015, 30, 44-52.

Table 1

Crystal and experimental data of norethisterone enanthate

Empirical formula	$C_{27}H_{38}O_3$
Formula weight	410.57
Temperature/K	110.01(16)
Crystal system	orthorhombic
Space group	$P2_12_12_1$
a/Å	6.09236(14)
b/Å	12.7347(3)
c/Å	30.1234(8)
α/°	90
β/°	90
γ/°	90
Volume/Å^3	2337.10(10)
Z	4
ρ_{calc}g/cm^3	1.167
μ/mm^{-1}	0.576
F(000)	896.0
Crystal size/mm^3	0.4 × 0.4 × 0.3
Radiation	CuKα (λ = 1.54184)
2θ range for data collection/°	9.094 to 134.13
Index ranges	-5 ≤ h ≤ 7, -9 ≤ k ≤ 15, -37 ≤ l ≤ 33
Reflections collected	8339
Independent reflections	3936 [R_{int} = 0.0312, R_{sigma} = 0.0405]
Data/restraints/parameters	3936/0/273
Goodness-of-fit on F^2	1.058
Final R indexes [I>=2σ (I)]	R_1 = 0.0543, wR_2 = 0.1376
Final R indexes [all data]	R_1 = 0.0569, wR_2 = 0.1404
Largest diff. peak/hole / e Å^{-3}	0.31/-0.32
Flack parameter	-0.26(15)

Table 2 Selected bond lengths (Å) and angles (˚) of NET-EN and corresponding parameters of NET-AC

NET-EN		NET-AC[32]
O(1)–C(10)	1.352(3)	1.355(7)
O(1)–C(17)	1.451(3)	1.458(5)
O(2)–C(10)	1.202(4)	1.202(7)
C(6)–C(14)	1.187(4)	1.176(7)
C(26)–C(28)	1.486(6)	1.482(7)
C(26)–O(3)	1.204(5)	1.234(6)
C(26)–C(30)	1.475(5)	1.450(8)
C(7)–C(30)	1.337(4)	1.348(7)
O(1)–C(10)–C(19)	111.7(2)	109.2(6)
O(1)–C(17)–C(6)	109.6(2)	108.7(4)
C(14)–C(6)–C(17)	177.8(3)	179.4(5)
O(1)–C(17)–C(8)	107.7(2)	107.1(3)
O(1)–C(17)–C(18)	113.5(2)	113.4(4)
C(6)–C(17)–C(18)	110.7(2)	111.5(4)
C(6)–C(17)–C(8)	112.2(2)	112.4(4)
C(8)–C(17)–O(1)–C(10)	171.8(2)	172.9(5)
C(18)–C(17)–O(1)–C(10)	58.5(3)	59.2(6)
C(17)–O(1)–C(10)–O(2)	2.6(4)	-0.6(9)
C(17)–O(1)–C(10)–C(19)	-177.1(2)	179.9(5)

Table 3

Stern-Volmer quenching constants for NET-EN-HSA interaction

T/K	K_{SV} ($Lmol^{-1}$)	R^a
298	$(1.015 \pm 0.0023) \times 10^4$	0.9981
310	$(6.581 \pm 0.0167) \times 10^3$	0.9944
315	$(5.826 \pm 0.0094) \times 10^3$	0.9968

[a] the correlation coefficient for the K_{sv} values.

Table 4

Lifetimes of fluorescence decay of HSA in Tris-HCl of pH 7.4 at different concentrations of NET-EN.

System	c(drug) ($\times 10^{-5}$ mol·L^{-1})	τ_1	τ_2	α_1	α_2	‹τ›	χ^2
Free HSA	0.0	2.311	6.702	0.099	0.901	6.267	1.044
	1.6	1.427	6.336	0.117	0.883	5.762	1.139
NET-EN−HSA	3.2	0.626	6.074	0.085	0.915	5.611	1.173
	4.8	0.349	5.921	0.069	0.931	5.537	1.219

Table 5

Binding constants K, binding sites n, and thermodynamic parameters for NET-EN-HSA interaction

T/K	K ($Lmol^{-1}$)	n	R^a	ΔG^0 (kJ·mol^{-1})	ΔH^0 (kJ·mol^{-1})	ΔS^0 (J·mol^{-1})	R^b
298	$(1.053 \pm 0.0035) \times 10^4$	1.002	0.9967	−22.93			
310	$(7.061 \pm 0.0207) \times 10^3$	1.004	0.9935	−22.91	−23.43	−1.667	0.9960
315	$(6.394 \pm 0.0136) \times 10^3$	1.007	0.9971	−22.90			

[a] is the standard deviation for the K values.

[b] the correlation coefficient for the van't Hoff.
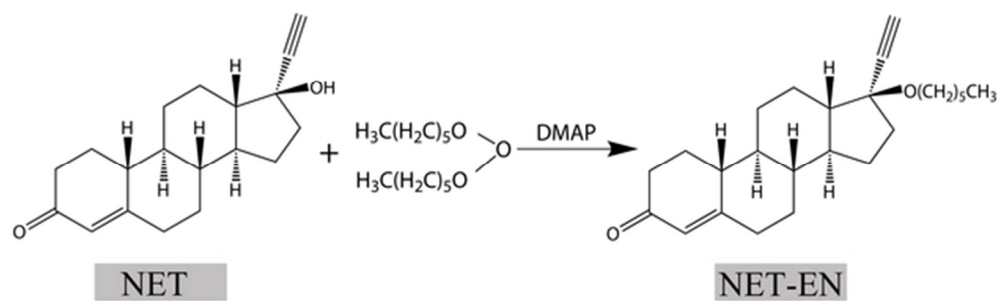
Fig. 1. Synthesis route of NET-EN.
26x8mm (600 x 600 DPI)
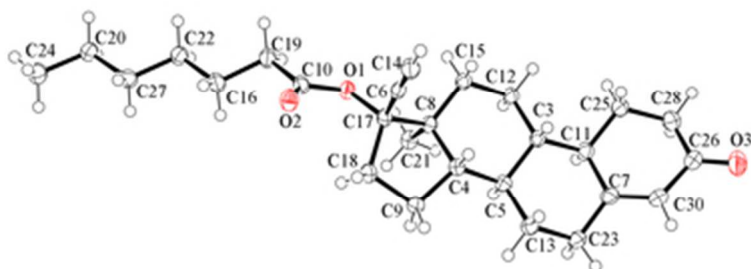
Fig. 2. Molecular structure of NET-EN showing the atom-numbering scheme.
33x13mm (300 x 300 DPI)
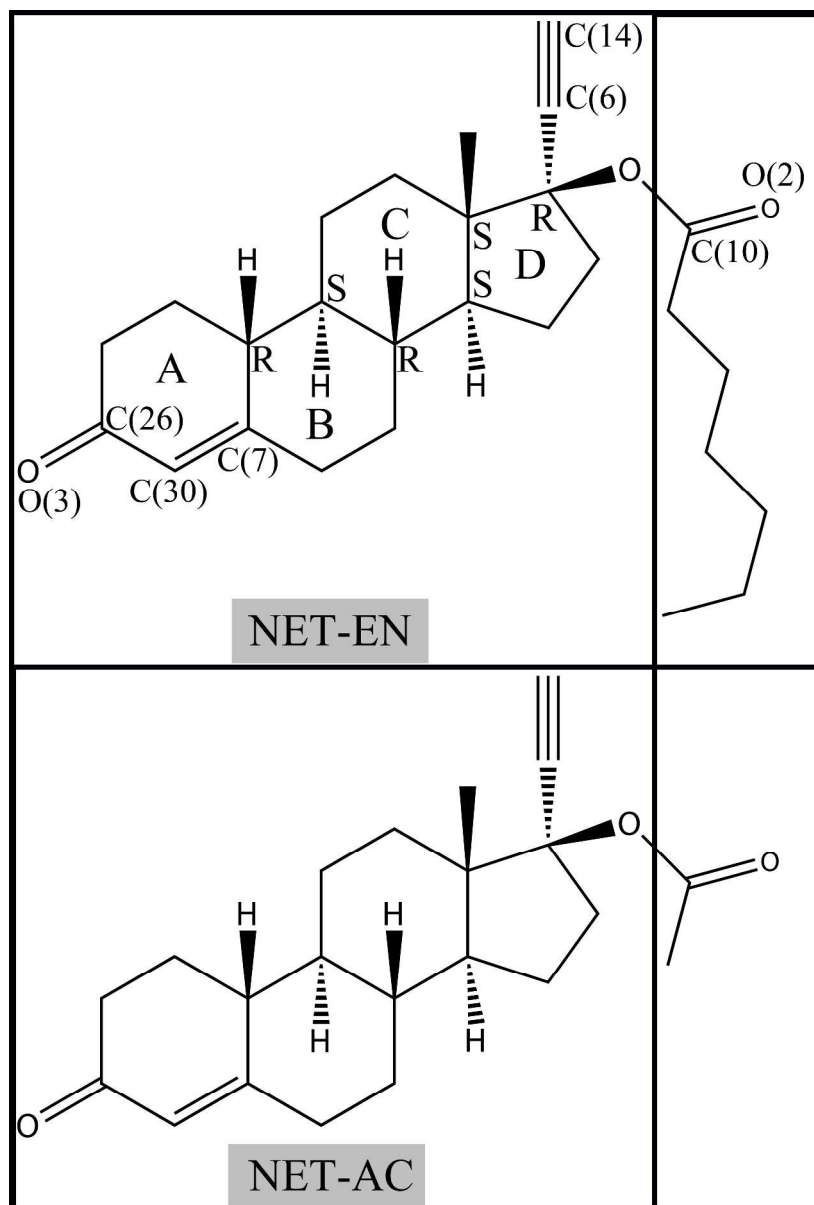
Fig. 3. Molecular structures of NET-EN and NET-AC.
149x220mm (600 x 600 DPI)
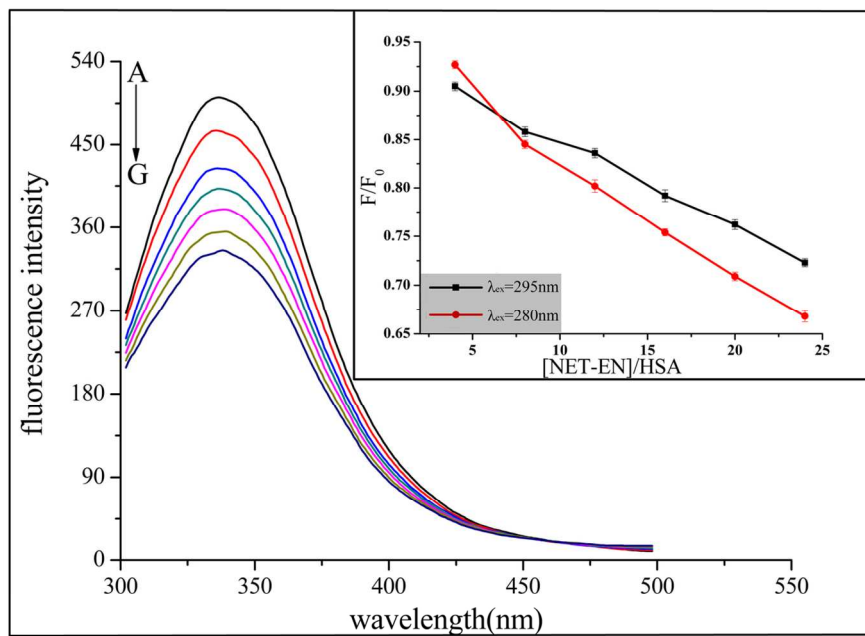
Fig. 4. Fluorescence spectra of HSA in the presence of NET-EN at 298 K. HSA concentration was 2 μM (A). NET-EN concentrations were 8 (B), 16 (C), 24 (D), 32 (E), 40 (F), and 48 μM (G). The inset was the quenching curve of the HSA in the presence of NET-EN obtained for 280 and 295 nm excitation wavelengths. 62x47mm (600 x 600 DPI)
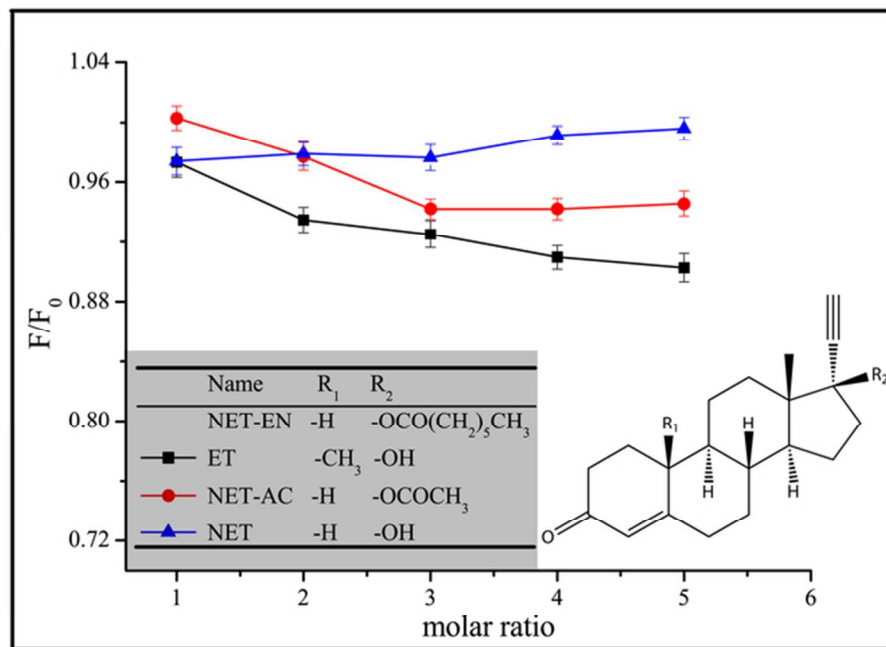
Fig. 5. Effect of distractors on the fluorescence of NET-EN-HSA complexes. C(NET-EN) =C(HSA)= 2.0 μM. The molar ratios of distractors to NET-EN-HSA complexes were 1:1, 2:1, 3:1, 4:1, and 5:1.
62x47mm (300 x 300 DPI)
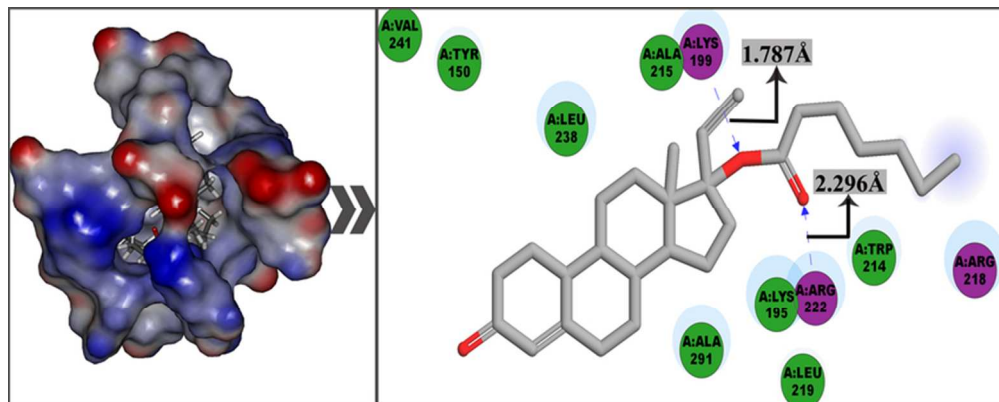
Fig. 6. Molecular docking simulation results by using DS3.1: Panel a: Surface around NET-EN in site 1. Panel b: 2D docking mode between NET-EN and HSA. Only important interacting residues are shown and represented as sticks. The hit compound is shown in pink. Residues involved in hydrogen bonding, charge, and polar interactions are represented by magenta circles. Residues involved in van der Waals interactions are represented by green circles. The solvent-accessible surfaces of atoms are represented by a blue halo around the atom. The diameter of the circle is proportional to the solvent accessible surface. Hydrogen bonding interactions with amino acid side chains are represented by a blue dash with the arrows directed toward the electron donor.
71x28mm (300 x 300 DPI)
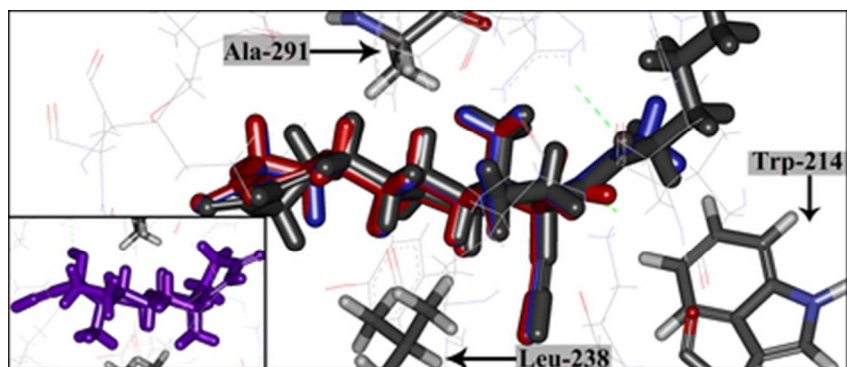
Fig. 7. Superimposition of docked poses of NET-EN (black), NET-AC (blue), and NET (red) in the site 1 of HSA. The inset was the docked pose of ET (purple).
35x15mm (300 x 300 DPI)
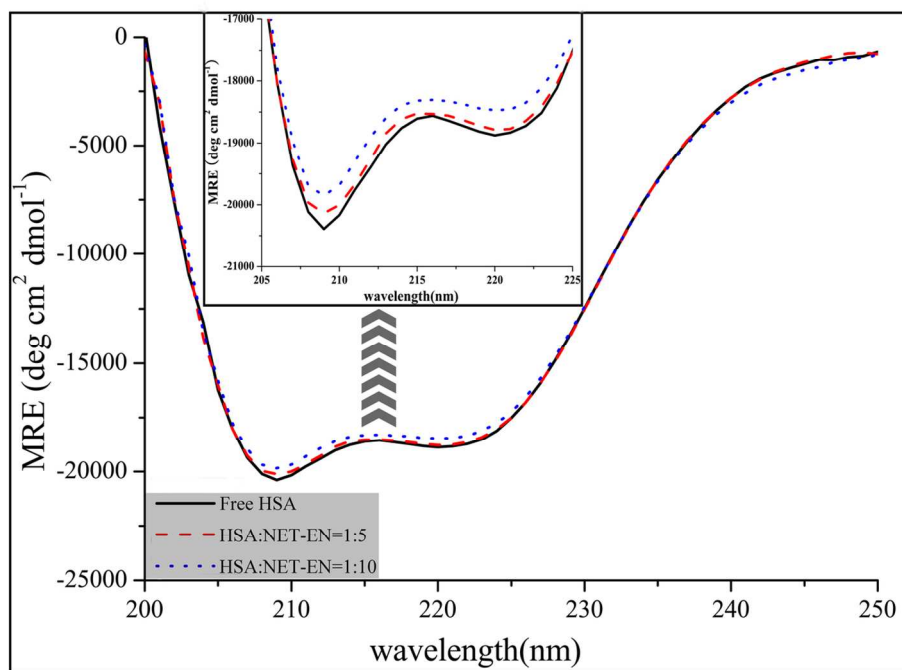
Fig. 8. Circular dichroism (CD) spectra of free HSA (2.0 µM) and HSA complex with NET-EN (ri = [HSA]/[NET-EN] =1:5, 1:10) at pH 7.40.
63x48mm (600 x 600 DPI)
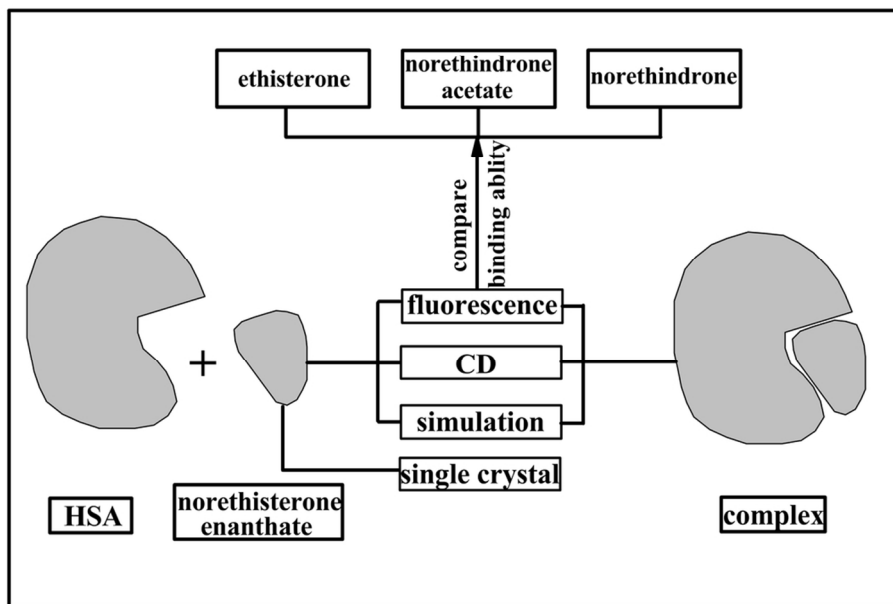
Graphical abstract: Fatty acid ester norethisterone enanthate binding to human albumin
49x35mm (600 x 600 DPI)